14th Annual International Conference on Industrial Engineering and Operations Management Dubai United Arab Emirates (UAE), February 12-14, 2024

Publisher: IEOM Society International, USA
Published: February 12, 2024
DOI: 10.46254/AN14.20240036

Taguchi-GRA Application in Multi-objective Optimization of FSP Variables for AA8011/TiC Composite

Pankaj Chandna
Professor, Mechanical Engineering Department
National Institute of Technology Kurukshetra
Haryana 136119, India
pchandna08@gmail.com

Raman and Pawan Bishnoi
Research Scholar, Mechanical Engineering Department
National Institute of Technology Kurukshetra
Haryana 136119, India
rmnchauhan06@gmail.com, er.pawan27@gmail.com

Abstract

Research on Aluminum Matrix Composites has seen an exponential growth in the recent past, as the qualities demonstrated by metal matrix composites are far more appealing than those of unreinforced metals. Many properties, such as high-temperature strength, high elastic modulus, greater stiffness, creep, and fatigue resistance, make them more significant for automotive and aerospace applications. Friction Stir Processing (FSP) has gained importance for surface generation because it does not influence the parent properties of the material. The component's surface is cardinal for many applications, and the product's life depends on surface properties such as wear resistance, etc. In this work, FSP has been used to create an AA8011/TiC surface composite, and the effect of process parameters, including tool rotational speed, linear movement of the tool, and dwell duration, on various surface attributes have been investigated. Taguchi-based Grey Relational Analysis (TGRA) has been employed to develop distinct sets of process parameters and optimize the response parameters simultaneously. After analyzing the obtained optimum results, it is concluded that TiC can be utilized as a reinforcement. FSP has proven to be a good option for producing AA8011/TiC surface composites. The optimal parametric setting for maximization of microhardness and grain number was 1000 RPM of tool rotation speed, 25 mm/min linear speed, and 35 seconds of dwell duration. The surface composite layer generated by the FSP process exhibits better results for both responses than the AA8011 sheets, as received.

Keywords

FSP, GRA, Taguchi, AA8011, and AMC

1. Introduction

Aluminum Matrix Composite (AMC) products are lower in weight, have sufficient strength and mechanical qualities, and resist wear and corrosion (Dinaharan et al., 2020; Thangarasu et al., 2014b). AMCs find colossal applications in fabricating armour in the defence sector due to their high strength-to-weight ratio. The automotive industry is also interested in AMC due to its ease of machinability and overall appealing polished appearance (Ramnath et al., 2014). Aluminum can incorporate assorted reinforcing particles, and the effects are highly productive (Aynalem, 2020).

The FSP principle (Figure. 1) allows inserting a pin profile or tool shoulder into the work material by applying an axial force to the tool and then moving the tool along the pre-set path at an altering traverse speed. Several tool geometries and tool movements are used to achieve the desired results. The friction created by the tool's relative

movement generates heat, causing the work material to deform and migrate down the pin profile. The frictional temperature must be less than the melting point of the base plate material and sufficient to plasticize the material for smooth movement along the pin profile (McNelley, 2010; Mishra et al., 2003). The applications of FSP on Metal Matrix Composites have received significant attention from researchers in recent years.

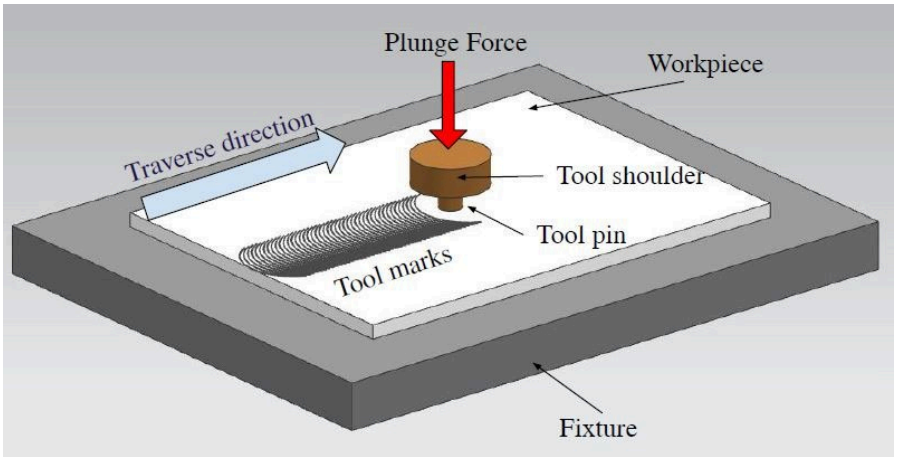

Figure 1. Schematic view of FSP setup

Most of the reported research works reveal many benefits of surface treatment using the FSP technique over conventional surface treatment methods. Some of these have been discussed here. Barmouz and Givi exercised multiple-pass FSP with 100 % overlapping to enhance the microstructural and mechanical characteristics of Cu/SiC composites. Optimal traverse and rotational speeds were 40mm/min and 900 rpm. The results showed that the hardness after the first, fourth, and eighth passes improved by about 30%, 50%, and 60%, respectively (Barmouz and Givi, 2011). Rayes and Danaf studied the influence of multiple passes on FSP. AA6082-T651 sheets with varying linear speeds were used for the experimental work; it was concluded that a rise in transverse speed and more FSP passes led to better grain size growth and high hardness (El-Rayes and El-Danaf, 2012). Shahraki et al. AA5083/ ZrO_2 nanocomposite layer was fabricated through FSP. It was found that the distribution of reinforcement material at high and low traverse speeds was not adequate (Shahraki et al., 2013). Thangarasu et al. evaluated the effect of the insertion of TiC particles to create AA6082/TiC surface composite through FSP; homogenous dispersion of reinforcement particles was observed, and a rise in the amount of TiC powder gave rise to better microhardness and UTS of the material (Thangarasu et al., 2014a). Hashemi and Hussain focused on fabricating the Al7075-T65/TiN surface composite layer with the help of FSP. The threaded tool with four passes produced a 60 % higher wear resistance and 45 % lower friction coefficient (Hashemi and Hussain, 2015). Adetunla and Akinlabi experimented to increase the work life of AA1100 by increasing wear resistance by fabricating Al/Ti-6Al-4V surface composite (Adetunla and Akinlabi, 2018). Vijayavel and Balasubramanian exposed that the tool with a tapered columnar probe profile fashioned a defect-free surface with higher hardness and wear resiliency than other probe profiles (Vijayavel and Balasubramanian, 2018). Khodabakhshi et al. studied the factors influencing the cold spray process for submission on Pure Ti coating on AA5083. The results show grain size reduction up to values less than 1 µm. A 700 % increment in microhardness value was observed after the FSP compared to the hardness value of a cold-sprayed coated surface (Khodabakhshi et al., 2019). Patel et al. reported that lower temperatures prevented grain growth, and the final specimen reached superplastic elongation up to 572 % (Patel et al., 2019). Mourad et al. successfully fabricated a composite of Aluminum 6082 and Tungsten carbide as reinforcement material; they concluded that the composite's microhardness, UTS, and wear resiliency was significantly improved compared to the as-received parent material and the decrease in the wear rate of the output material (Mourad et al., 2020). Dinaharan et al. concluded that UTS was increased from 226 MPa to 283 MPa with Titanium powder in 0 and 21 volumetric percentages with AZ31 alloy, respectively (Dinaharan et al., 2020). Viswanathan et al. focused on improving the wear resistance of AA7075 composite reinforced with SiC particles with the help of FSP. Results showed a slow rise in wear rate alongside the increase in force applied from 10 N to 30 N (Viswanathan et al., 2021).

The authors have felt that less work has been reported on Al/TiC composites; however, it requires more attention from the researchers due to its broader applications, including aerospace, automotive, biomedical, electronics sector, etc.

The present work aims to optimize the FSP process parameters, tool rotational speed, linear speed, and dwell time simultaneously to maximize the microhardness and get higher grain numbers for the FSPed sheets of Al/TiC using TGRA.

2. Methods

The rectangular sheets of AA8011 with dimensions of 150 mm x 150 mm x 5mm have been utilized as the workpiece in this work. Every sheet of AA8011 has two grooves etched using a slotter machine, each having a depth of 2 mm and a width of 1 mm. The elemental composition with the XRD analysis of the AA8011 sample has been depicted in Figure 2. Emery paper was used to remove the oxide layer before the analysis, and the sample was then cleaned with ethanol. Aluminum 8011 alloy has a 2.71 g/cm3 density, thermal conductivity of 237 W/m-K, and tensile and yield strengths of 150 and 115 MPa, respectively. The reinforcing powder used in this research is a TiC alloy powder. TiC powder has an average particle size of 2 µm, and its chemical composition and characteristics are reported in Table 1.

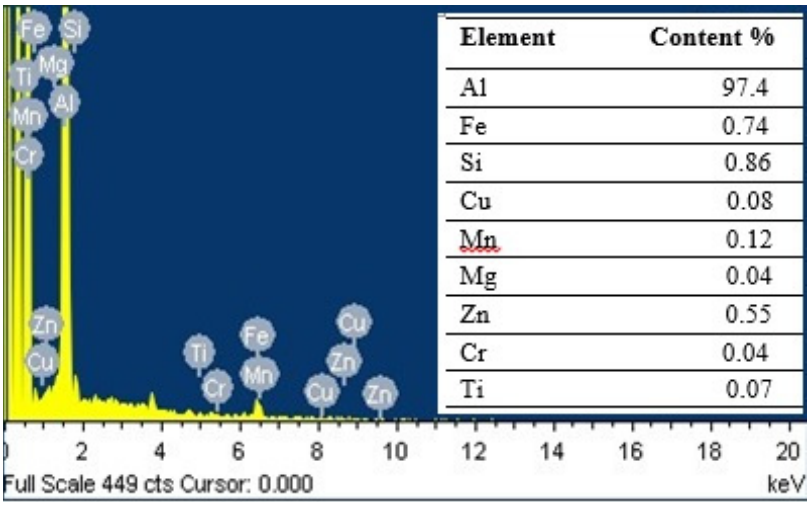

Figure 2. XRD Analysis of AA8011 Sample

Table 1. Chemical composition and properties of reinforcement material

Total C	**Free C**	**Nb**	**Fe**	**Impurities (max %) Si**	**O**	**N**	**Na**	**K**	**Ca**
≥19.1	≤0.30	0.01	0.05	0.02	0.5	0.2	0.01	0.005	0.01
Properties of reinforcement material (TiC powder)									
Properties			**Metric**				**Imperial**		
Melting Temperature			3150 °C				5725 °F		
Boiling Temperature			4825 °C				8700 °F		
Density			4.94 g/cm^3				0.177 lb/in^3		

The material has the surface frictional characteristics to generate enough heat for the FSP process to mix the TiC powder into the 8011 sheets to form the alloy mixture. Figure 3 depicts the FSP tool utilized for this experiment. TiC powder (25% fractional volume) has been uniformly mixed with alcohol and put into the grooves. The plates were then placed in an airtight container to prevent air bubbles from becoming caught in the filling. Three process variables, tool rotational per minute (RPM), linear speed (LS), and dwell time, were chosen based on trial tests for the current investigation. Linear speeds of 16 mm/min, 20 mm/min, and 25 mm/min, rotational speeds of 710, 1000, and 1400 rpm, and dwell times of 25, 30, and 35 seconds were used. Each FSP sample is subjected to three passes with 100% overlap. After each pass, the initial plunge depth of 0.2 mm increased by 0.05 mm. The trials have been

carried out on a vertical milling machine provided at NIT, Kurukshetra. The FSP setup is comprised of a mild steel fixture. Bolts hold the AA8011 plate to the fixture.

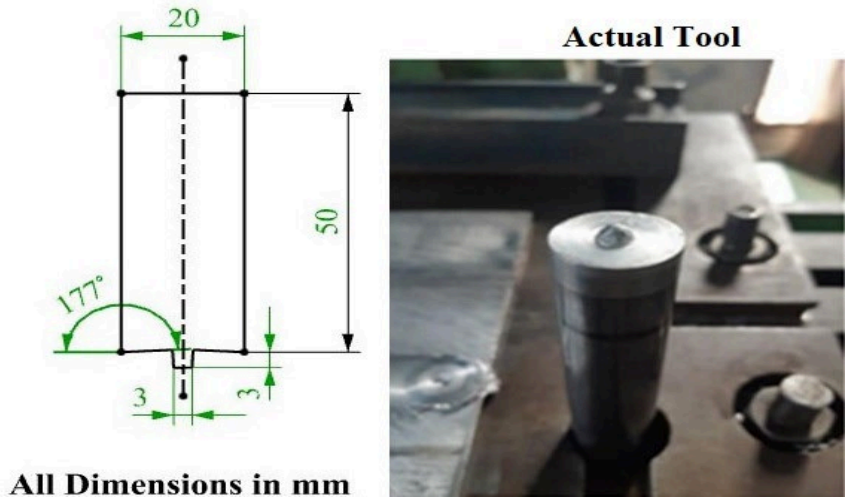

Figure 3. The FSP Tool used in the experiment

2.1 Measurement of Microhardness

After the experiment, specimens were cut for sample preparation to analyze the microhardness of the prepared surface, as shown in Figure 4. Each sample was polished using emery paper to make it appear mirror-like. Vickers's Microhardness Tester with a diamond indenter has been used to conduct the microhardness testing. A 200 g load with a dwell period of 15 seconds has been used. Each sample obtained readings at three locations: the stir zone, the heat-affected zone, and the thermo-mechanically impacted zone. The mean of these three values has been used to get the individual specimen's final microhardness value. The microhardness of AA8011 has been measured as 215 HRV.

Figure 4. Samples for Microhardness Test

2.2 Measurement of Grain Number

The microstructural investigation was performed using an Olympus BX51M microscope. The samples were prepared and groomed following the ASTM standard. Kroll's reagent was used to prepare the pieces before the examination. The reagent has been produced from 100 mL distilled water, 2 mL HF, and 4 mL NHO3. After around 30 seconds of etching, samples were inspected to evaluate the grain size of the composite layer formed on the AA8011 plates. The Grain number for the parent material is 6.34.

3. Results and Discussions

3.1 Analysis of Experimental Results for Microhardness

Table 2 depicts microhardness and grain number values obtained after experimentation according to the Taguchi L9 Orthogonal array.

Table 2. Responses corresponding to experimental design

Serial No	RPM [RPM]	LS [mm/min]	Dwell Time [s]	Microhardness [HRV]	Grain Number
1	710	16	25	268.3	7.22
2	710	20	30	320.2	7.64
3	710	25	35	360.7	7.98
4	1000	16	30	298.6	7.34
5	1000	20	35	390.4	7.90
6	1000	25	25	341.3	7.80
7	1400	16	35	262	7.40
8	1400	20	25	259.3	7.42
9	1400	25	30	281.2	7.62

3.1.1 Effects of RPM

Figure. 5 shows the major effect plots for means of microhardness samples generated by FSP at various rotational speeds, traverse speeds, and dwell periods. An increase in tool rotation speed aids in the uniform circulation of these reinforcing units. The graph shows that microhardness increases as RPM increases from 710 to 1000 RPM. The RPM of the FSP tool controls the amount of heat given inside the processed zone, which disrupts the microstructure within the matrix and the material's final qualities. TiC powder began to diffuse out of the groove after 1000 RPM during the experiment. As a result of the heat generated by the increase in RPM beyond 1000 RPM, the microhardness value decreased.

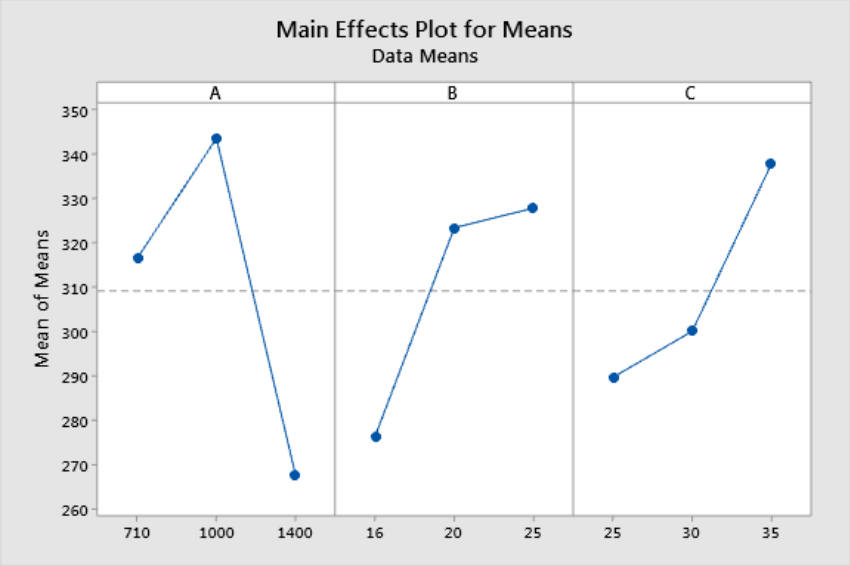

Figure 5. Microhardness Variation with RPM; LS; Dwell Time

3.1.2 Effects of LS

The increasing hardness with increasing LS can also be related to the fact that an increase in linear speed directs a decrease in the length of exposure to the heat produced during the operation, resulting in TiC not being diffused

uniformly and failure in cluster breakup. The idea is to reduce the tool's rotating speed to achieve higher microhardness values while increasing its linear speed. This toughest sample has been obtained at a rate of 25 mm/min LS. Higher traverse speed also implies less exposure to the heat generated during the activity.

3.1.3 Effects of Dwell Time

The FSP process begins by delivering a specific rotating speed to the FSP tool, followed by a fixed plunge depth into the metal sheet and circling the tool at the particular position for a period known as dwell time. With the parameter set at three levels, it has been discovered that increasing the dwell duration promotes the intensification of the microhardness value. The dwell time completes the process by producing enough heat for the material to deform plastically. This aids in grain refinement because dense dislocation and finer grains promote microhardness. In other words, cold working or work hardening occurs with the assistance of dwell time, which supports the increase in microhardness value. The slope of the graph between the 30s and 35s is higher than the slope between the 25s and 30s because the slope represents the rate at which work hardening occurs; thus, the higher the hill, the greater the work hardening.

3.2 Analysis of Experimental Results for Grain Number

Elevated temperature during the FSP and the material's plastic deformation produced minute-equated structures in the treated zone. Phenomena such as Dynamic Recovery, Discontinuous dynamic recrystallization, and Geometric dynamic recrystallization are responsible for grain refinement during FSP.

3.2.1 Effects of RPM

As illustrated in Figure 6, Because of the reinforcing particles present in the metal matrix, a rise in RPM increased the grain number; this can be seen in the graph for RPM values ranging from 710 to 1000. As previously stated, TiC powder can reduce grain growth to a certain extent. After 1000 rpm, particles began to disperse outside the metal sheet, and the effect of high temperature caused by tool rotation became apparent. After 1000 rpm, the grain number began to decline.

Figure 6. Grain Number variation with Rpm, LS; Dwell Time

3.2.2 Effects of LS

The greater the LS, the shorter the period for which the tool rotated at a given position. The graph showed that the grain number increased as the linear speed increased. Grain growth recrystallization slows as traverse speed increases; thus, that specific area has been exposed to the heat created during the operation for a shorter time. When the slope of LS was compared between 16 mm/min and 20 mm/min and 20 mm/min to 25 mm/min, it was clear that the pitch became less sensitive. It occurs because the role of TiC powder in grain refining becomes less critical as traverse speed increases.

3.2.3 Effects of Dwell Time

The goal of allowing dwell time is to plasticize the material at the beginning of the process. As dwell time increases, more grain refining occurs at the start of the process. The graph shows that the chart gets more sensitive as dwell time grows. That happens because, as dwell time increases, TiC powder begins to break at the beginning of the process; if this continues, the pinning effect enters the picture, and the grain refinement rate increases.

3.3 Grey Relational Analysis and Optimum Parameters

The TGRA implementation for the simultaneous optimizations of microhardness and grain number for FSP of AA8011/TiC includes the following steps.

3.3.1 Computation of the S/N Ratios

The fundamental stage in TGRA is the computation of the S/N ratio of linked responses using the rules tabulated in Table 3. In table y_i is the response data. According to the current optimization problem, both responses are to be maximized, so the larger is better approach is used to compute S/N ratios (Raju and Sathiya Narayanan, 2016).

Table 3. S/N ratio computation rules

Approach	Objective	Data Characteristics	Equations
Smaller is better	Minimize the response	Non-negative with zero as the target	$\frac{S}{N_S} = -10\,log\left(\frac{1}{n}\sum_{i=1}^{n} y_{ij}^2\right)$
Larger is better	Maximize the response	Positive	$\frac{S}{N_L} = -10\,log\left(\frac{1}{n}\sum_{i=1}^{n} \frac{1}{y_{ij}^2}\right)$

3.3.2 Computation of Normalized Values for S/N Ratios

The next stage in GRA is normalizing the considered S/N ratio after computing the S/N ratio for related responses. Data normalization is necessary because the units and ranges in a single data series may differ from those in others. Thus, data is normalized by converting the original order into an analogous sequence. The y_{ij} is transformed into an analogous sequence by the given formula for a larger-the-better approach.

$$Z_i = \frac{y_{ij} - y_{lowest}}{y_{highest} - y_{lowest}}$$

The computed S/N ratio and normalized values are tabulated in Table 4.

Table 4. Computed S/N ratio and normalized values

Run No.	S/N Ratio for Responses		Normalized Values for Responses	
	Microhardness	Grain Number	Microhardness	Grain Number
1	48.572	17.170	0.083	0.000
2	50.108	17.661	0.515	0.564
3	51.142	18.040	0.806	1.000
4	49.501	17.313	0.344	0.164
5	51.830	17.952	1.000	0.899
6	50.662	17.841	0.671	0.772
7	48.366	17.384	0.025	0.246
8	48.276	17.408	0.000	0.273
9	48.980	17.639	0.198	0.538

3.3.3 Computation of Grey-Relational-Coefficients (GRCs)

For the calculation of GRC, the following formula is used.

$$GRC_{ij} = \frac{\Delta_{lowest} + \mu_{\Delta_{highest}}}{\Delta_{ij} + \mu_{\Delta_{highest}}}$$

Where μ is the weight assigned to individual responses; μ is taken as 0.5 (Sindhu et al., 2019).

3.3.4 Computation of Grey-Relational-Grades (GRGs)

The GRG is calculated using the formula

$$GRG_i = \frac{1}{r}\sum GRC_{ij}$$

Where r = number of responses. The GRC, GRG, and rank of each experimental run are computed and reported in Table 5.

Table 5 Computed GRCs, GRGs, and Rank

Run No.	GRC for responses		GRG	Rank
	Microhardness	Grain Number		
1	0.352	0.333	0.343	9
2	0.507	0.534	0.521	4
3	0.721	1.000	0.860	2
4	0.432	0.374	0.403	6
5	1.000	0.832	0.916	1
6	0.603	0.686	0.645	3
7	0.339	0.398	0.368	8
8	0.333	0.407	0.370	7
9	0.384	0.520	0.452	5

3.4 Finding the Optimum Parametric Setting

The final stage is to forecast and check the enhancement of the response by using the optimal level of FSP parameters. By using optimum settings of FSP parameters, the projected GRG may be computed as follows:

$$GRG_p = GRG_m + \sum_{i=0}^{p} GRG_i - GRG_m$$

where, GRG_p = projected GRG; GRG_m = GRG mean; p = number of FSP parameters.

Taguchi's analysis of GRGs has been conducted in Minitab 19 software to find the optimum parameter settings. The obtained main effect plots for GRG are depicted in Figure 7, the response table for GRG is reported in Table 6 (optimum levels are bolded), and the ANOVA table for GRG has been reported in Table 7, which shows the optimum parameter settings is at 1000 RPM, 25 mm/min linear speed and 35 s dwell time. The linear speed is the most significant parameter, and tool RPM was the least important parameter, with dwell time as an intermediate considerable parameter. The confirmatory experiments have been conducted in this setting; the outcomes are reported in Table 8. The results show improvement in the responses, and the error between predicted and measured values are within permissible limits.

Figure 7. Main effects plots for GRG

Table 6. Response Table for GRG

Level	RPM	LS	Dwell Time
1	0.5750	0.3719	0.4529
2	**0.6550**	0.6026	0.4590
3	0.3971	**0.6526**	**0.7152**
Delta	0.2579	0.2807	0.2623
Rank	3	1	2

Table 7. ANOVA table for GRG

Source	DF	Adj SS	Adj MS	F-value	*p*-Value	Contribution
RPM	2	0.104532	0.052266	20.13	0.047	27.60%
LS	2	0.134547	0.067273	25.90	0.037	35.52%
Dwell Time	2	0.134473	0.067237	25.89	0.037	35.50%
Error	2	0.005194	0.002597			1.37%
Total	8					100.00%

Table 8. Outcomes of Confirmatory Experiments

Primary settings		**Optimum settings**		
RPM 1000; LS 20mm/min; Dwell Time 35s		RPM 1000; LS 25mm/min; Dwell Time 35s		
Response	**Actual values**	**Predicted values**	**Actual values**	**Error %**
Microhardness (HRV)	390.4	390.64	398.7	2.06
Grain Number	7.90	8.05	8.23	2.23

4. Conclusions

The Taguchi method has applied an orthogonal array of nine sets for process parameters, such as rotational speed, linear speed, and dwell time, to create nine specimens. After analyzing these specimens, it has been stated that TiC could be utilized as a reinforcement material for creating an AA8011/TiC surface composite layer. From the analysis of the experimental data, the following can be concluded:

- ✓ A rise in spindle speed up to 1000 rpm from 710 rpm helps increment the microhardness value. Further increments in spindle speed caused the dispersion of reinforcement units far from the metal matrix; hence, the microhardness value decreased with the rise of spindle speed between 1000 rpm and 1400 rpm.
- ✓ An increase in the traverse speed and dwell time helps increment grain numbers, and as a result, the microhardness value also increases with the rise in LS and dwell time value.
- ✓ Dwell time helps in the mixing of TiC powder in the initial stages of the FSP process and gives a start for the smooth run of tool movement along the predefined processing zone.
- ✓ ANOVA analysis of the output results helps to deduce the role of the selected input parameters, and the results showed that all three parameters were significant.
- ✓ The maximum microhardness and highest grain number values have been obtained at 1000 rpm, 25 mm/min, and 35 s dwell time using TGRA.
- ✓ The microhardness improved from 215 HRV to 398.7 HRV, and the grain number improved from 6.34 to 8.23.
- ✓ Traverse speed and RPM influenced the distribution of reinforcement and TiC particles. Higher RPM and LS values resulted in TiC particle circulation outside the metal matrix.
- ✓ The surface composite layer generated by the FSP process exhibits better microhardness and grain number results than the as-received A8011 sheet.

Based on their findings during the trials, the authors believe that utilizing a thin strip of aluminum to prevent TiC powder dispersion beyond the metal matrix could be helpful in future studies. Additionally, with the reinforcing material placed inside the grooves, the TIG cladding process on the profile can be done to produce the initial bond between the TiC particles and base metal. Instead of grooves, holes can be drilled, and reinforcement particles can be placed inside the drilled holes to improve TiC-base material mixing.

References

Adetunla, A. and Akinlabi, E. Mechanical characterization of Al/Ti-6Al-4V surface composite fabricated via FSP: A comparison of tool geometry and number of passes, *Materials Research Express*, vol. 5, no. 11, 115015, 2018.

Aynalem, G. F. Processing Methods and Mechanical Properties of Aluminium Matrix Composites, *Advances in Materials Science and Engineering*, vol. 2020.

Barmouz, M. and Givi, M. K. B. Fabrication of in situ Cu/SiC composites using multi-pass friction stir processing: Evaluation of microstructural, porosity, mechanical and electrical behavior, *Composites Part A: Applied Science and Manufacturing*, vol. 42, no. 10, 1445–53, 2011.

Dinaharan, I., Zhang, S., Chen, G., and Shi, Q. Titanium particulate reinforced AZ31 magnesium matrix composites with improved ductility prepared using friction stir processing, *Materials Science and Engineering: A*, vol. 772, 1–11, 2020.

El-Rayes, M. M. and El-Danaf, E. A. The influence of multi-pass friction stir processing on the microstructural and mechanical properties of Aluminum Alloy 6082, *Journal of Materials Processing Technology*, vol. 212, no. 5, 1157–68, 2012.

Hashemi, R. and Hussain, G. Wear performance of Al/TiN dispersion strengthened surface composite produced through friction stir process: A comparison of tool geometries and number of passes, *wear*, vols 324–325, 45–54, 2015.

Khodabakhshi, F., Marzbanrad, B., Shah, L. H., Jahed, H., and Gerlich, A. P. Surface Modification of a Cold Gas Dynamic Spray-Deposited Titanium Coating on Aluminum Alloy by using Friction-Stir Processing, *Journal of Thermal Spray Technology*, vol. 28, no. 6, 1185–98, 2019.

McNelley, T. R. Friction stir processing (FSP): refining microstructures and improving properties, *Revista de Metalurgia*, vol. 46, no. Extra, 149–56, 2010.

Mishra, R. S., Ma, Z. Y., and Charit, I. Friction stir processing: A novel technique for fabrication of surface composite, *Materials Science and Engineering: A*, vol. 341, nos. 1–2, 307–10, 2003.

Mourad, A., Mousa, E., and Kandil, A. Fabrication of Aa6082/Wc Nanocomposite By Friction Stir Processing and Optimization Using Taguchi Approach, *Journal of Al-Azhar University Engineering Sector*, vol. 15, no. 57, 1030–39, 2020.

Patel, V., Badheka, V., Li, W., and Akkireddy, S. Hybrid friction stir processing with active cooling approach to enhance superplastic behavior of AA7075 aluminum alloy, *Archives of Civil and Mechanical Engineering*, vol. 19, no. 4, 1368–80, 2019.

Raju, C. and Sathiya Narayanan, C. Application of a hybrid optimization technique in a multiple sheet single point

incremental forming process, *Measurement: Journal of the International Measurement Confederation*, vol. 78, 296–308, 2016.

Ramnath, B. V., Elanchezhian, C., Annamalai, R. M., .Aravind, S., Atreya, T. S. A., Vignesh, V., and Subramanian, C. Aluminium metal matrix composites - A review, *Reviews on Advanced Materials Science*, vol. 38, no. 1, 55–60, 2014.

Shahraki, S., Khorasani, S., Abdi Behnagh, R., Fotouhi, Y., and Bisadi, H. Producing of AA5083/ZrO2 nanocomposite by friction stir processing (FSP), *Metallurgical and Materials Transactions B: Process Metallurgy and Materials Processing Science*, vol. 44, no. 6, 1546–53, 2013.

Sindhu, D., Thakur, L., and Chandna, P. Multi-objective Optimization of Rotary Ultrasonic Machining Parameters for Quartz Glass Using Taguchi-Grey Relational Analysis (GRA), *Silicon*, vol. 11, no. 4, 2033–44, 2019.

Thangarasu, A., Murugan, N., and Dinaharan, I. Production and wear characterization of AA6082-TiC surface composites by friction stir processing, *Procedia Engineering*, vol. 97, 590–97, 2014a.

Thangarasu, A., Murugan, N., Dinaharan, I., and Vijay, S. J. Influence of Traverse Speed on Microstructure and Mechanical Properties of AA6082-TiC Surface Composite Fabricated by Friction Stir Processing, *Procedia Materials Science*, vol. 5, 2115–21, 2014b.

Vijayavel, P. and Balasubramanian, V. Effect of pin volume ratio on wear behaviour of friction stir processed LM25AA-5%SiCp metal matrix composites, *Alexandria Engineering Journal*, vol. 57, no. 4, 2939–50, 2018.

Viswanathan, R., Saravanan, K. G., Balaji, J., Prabu, R., and Balasubramani, K. Optimization of wear and friction parameters in Aluminum7075 hybrid composite, *Materials Today: Proceedings*, vol. 47, 4449–53, 2021.

Biographies

Pankaj Chandna has been working as a Professor in the Department of Mechanical Engineering at National Institute of Technology Kurukshetra. His academic contributions include publishing more than one hundred research papers in International and National Journals/Conferences, supervision of 14 PhD scholars, and 45 M.Tech dissertations in the varied areas of Production & Industrial Engineering. In addition to the above, he has served/serving as a member of Editorial Boards & Reviewer of International/National journals, and Fellow/Member of reputed Professional organizations. He has completed three research projects and one patent to his credit.

Raman Chouhan is a Master's student in the Department of Mechanical Engineering at National Institute of Technology Kurukshetra. His research interest includes advanced machining processes.

Pawan Bishnoi is a Ph.D. student in the Department of Mechanical Engineering at National Institute of Technology Kurukshetra and received his Master's from the same institute. His research interests include metal forming processes and advanced machining processes.